# DATABASE BUILDING AND STATISTICAL METHODS TO PREDICT SAILING YACHTS HYDRODYNAMICS

**Lionel Huetz**, Marc Lombard Yacht Design Group, France, lionel.huetz@gmail.com
**Pierre Emmanuel Guillerm**, Ecole Centrale de Nantes, France, pierre-emmanuel.guillerm@ec-nantes.fr

**Abstract.** The model characterizing the hydrodynamic forces acting on a sailing yacht hull can be built using extensive tank testing or CFD computations carried out on the studied hull shape. Unfortunately, in most cases involving sailing yachts, time and money are limited and testing each hull at the required speeds and attitudes is impossible. The idea is then to rely on a hydrodynamic model gathering results on various hulls; able to describe the evolution of the hydrodynamic forces depending on the hull shape through geometrical variables. The building and calibration of this type of model requires numerous computations but once the model is built, this approach is very fast. Furthermore, these models can provide a better understanding of the trends than tests on isolated hull shapes since they contain the results on a whole database of hulls. This type of approach using meta-models can be used in various fields to produce lots of results in a very short time and a better understanding of the phenomena involved. This paper presents a methodology to produce the database, select the relevant explanatory variables and build the formulations in the context of sailing yachts hydrodynamics. The regressions allowing the prediction of the running attitude and forces are presented.

## NOMENCLATURE

| | | |
|---|---|---|
| ALA | Apparent leeway angle | (°) |
| $A_{HL}$ | Lateral area of immersed part of the hull | ($m^2$) |
| $A_X$ | Maximum section surface | ($m^2$) |
| BEI | Bow entry incidence | (°) |
| $B_{WL}$ | Waterline beam | (m) |
| $C_B$ | Block coefficient | |
| CBR | Relative camber | |
| $C_f$ | Friction coefficient | |
| $C_{flot}$ | Flotation coefficient | |
| $C_P$ | Prismatic coefficient | |
| $C_{Pfront}$ | $C_P$ of the hull in front of maximum section | |
| $C_X$ | Maximum section coefficient | |
| $\widetilde{F}$ | Non dimensional form of F | (N) |
| Fn | Froude number | |
| $L_{WL}$ | Waterline length | (m) |
| $L_T$ | Longitudinal position maximum draft | (m) |
| $L_X$ | Longitudinal position maximum section | (m) |
| $L_{CB}$ | Longitudinal position centre of buoyancy | (m) |
| $L_{CG}$ | Longitudinal position centre of gravity | (m) |
| R | Rocker angle | (°) |
| Roy | Running trim angle | (°) |
| $S_C$ | Static wetted surface of the bare hull | ($m^2$) |
| T | Draft | (m) |
| Trz | Running sinkage | (m) |
| $T_T$ | Immersion of transom | (m) |

## 1. INTRODUCTION

“Is it fast?” is certainly the most common question that arises when observing a sailing yacht at the dock or ship lines in a design office. Sailing yachts find their energy in the relative motion between air and water. Their behaviour is governed by the equilibrium between aerodynamic forces one side and hydrodynamic forces on the other side. The combined simulation of these forces is a challenge and finding the three dimensional attitude, tuning and speed of the yacht fulfilling the equilibrium condition between all the forces is even more complex; so complex that computational time is very far from matching designer’s needs. Furthermore, a fully coupled simulation would be very hard to interpret in a design perspective since very various physical phenomena are interacting and mixed in the simulation. As a result, the aerodynamics and the hydrodynamics are always treated separately. Velocity prediction programs (VPPs) gather the results of each model to find the equilibrium of the yacht and finally predict its speed and attitude. In the present work, we are dealing with the characterization of the hydrodynamic model.

### 1.1 CONTEXT

Various approaches can be used to define the hydrodynamic model of a yacht. Indeed, the model may characterize directly the behaviour of the appended hull or deal with the bare hull and its appendages separately. Then, the hydrodynamic forces decomposition and their coupling with the attitude of the yacht can be dealt with in various ways. Finally, a choice has to be made between a steady or unsteady approach.

The level of decomposition is one of the main issues ruling the equilibrium between accuracy, computational time and versatility; the higher the level, the faster the computations and versatility but the more restricting the hypothesis on the physical effects involved. In fact, each time a problem is split into simpler problems, hypothesis on the coupling between the latter are made. This may lead to a loss of accuracy but also to a better understanding of the different separated physical phenomena and an enlarged field of application.

Finding the right balance between a direct approach of complex phenomena and a reductionist approach dividing complex problems into simpler ones is a recurrent problem in applied science. Choices have to be made, based on expertise and practice. Several preliminary designs and yacht performance studies as well as numerical simulations and analysis of the existing state of the art predictions led to the following conclusions:

- Significant improvements can be made while remaining in a quasi static VPP approach based on the coupling of three separated mathematical models (hull model, appendage model and aerodynamic model). Quasi static refers to the fact that dynamic effects are not directly included.
- Some attitude variables (leeway, running trim and sinkage) have to be added to the models and the VPP to improve the overall accuracy by improving the coupling between the different models.

In this context, the accuracy of the prediction relies mainly on the accuracy of the three models characterizing separately the hydrodynamic behaviour of the bare hull (without appendages), of its appendages and the aerodynamic behaviour of the yacht.

The appendages are relatively well described by the lifting line theory implemented in most of the VPPs, especially for high aspect ratio foils used on most of the modern yachts. The bare hull behaviour is much more complex to predict. There are two main ways of characterizing the hydrodynamic properties of a hull.

The first one is to carry out some tests on the studied hull shape for different values of speed and attitude variables such as heel and leeway angles. The results of these tests are stored in a matrix giving the relation between these input variables on one side and the forces and running attitude of the boat (output variables) on the other side. The tests can be carried out on scaled models in towing tank facilities or using computational fluid dynamic (CFD) tools. These two methods have their advantages and drawbacks, but they share one main drawback, they are so expensive and time consuming that their use is extremely restricted.

The other method is to use a mathematical model that is able to approximate the matrix described before; each term depending on geometrical parameters describing the shape of the hull. Different methods can be followed to build this type of mathematical models.

Since the flow around a yacht hull is very complex, they are all based on empirical or semi empirical approaches, using experimental results databases or real scale measurements on various hull shapes. In some cases, specific experimental campaigns called systematic series are set in order to build mathematical models describing the behaviour of ship hulls.

Despite a lower accuracy, the approach based on mathematical models presents many advantages. Once it is built, its use is very fast and cheap, facilitating the comparison of very various hulls during the design phase. Furthermore, the mathematical analysis of a large database can provide a better understanding of the phenomena involved than isolated tank tests or numerical simulations since they contain the results on various hulls.

The most famous formulations able to predict the hydrodynamics of sailing yacht hulls are based on the Delft Systematic Yacht Hull Series [1], [2].

The limitations of these formulations have been discussed in a previous paper [3]. These articles showed that a more detailed characterization was needed to improve the performance prediction, especially the influence of heel, leeway and trim.

### 1.2 MOTIVATIONS

The goal of the present study is to produce valuable information for the naval architects involved in the design of sailing yachts. This encompasses an improved accuracy and sensitivity of the velocity prediction but also the understanding of the physics involved. Our goal is to make this work as intelligible as possible for the designer, to stimulate the intuition and creativity instead of trying to replace them. In other words, turn the question “is it fast?” into “why is it fast?”

This led to the following conclusions:

- Build a computational loop that will be as versatile as possible to generate large databases of numerical experiments such as systematic series.
- Define a methodology and statistical tools to identify the relevant geometrical variables and build new formulations to predict the hydrodynamic forces and running attitude of yacht hulls.
- Develop a specific VPP to implement the developed formulations with their additional variables, especially the running attitude of the yacht.

The previous paper [4] presented the first results of this work and we will present here a more detailed description of the key issues of the methodology, much more extended formulations and the first results of the developed VPP.

## 2. TOOLS

The building of a numerical database involves various types of computations, realized by several modules. The different tools that are used in the loop are presented hereafter.

### 2.1 LOOP MONITORING

Figure 1 describes the modules involved in the loop used to build the database. DOE stands for design of experiments and will be discussed in the next section.

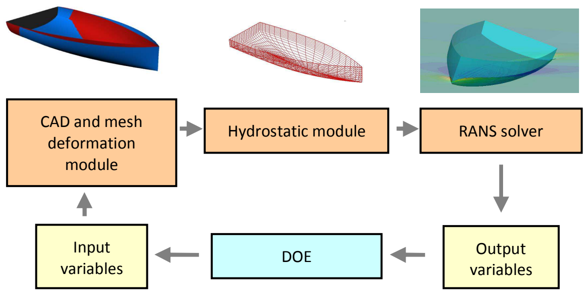


Figure 1: Chart of the loop

Input variables are:

- The parameters of the deformation used in the CAD module.
- The attitude variables (speed, yaw)

Outputs variables are:

- The hydrostatic coefficients.
- The hydrodynamic forces.

## 2.2 MORPHING TOOL

A morphing tool is used to generate various hulls and the associated volume meshes by deforming an initial hull and mesh. It is based on the hull modeller developed by HydrOcean as a plug in of Rhinoceros. This approach allows large changes in hull shapes without degrading the properties of the initial structured volume mesh. Figure 2 presents a zoom on the boundary layer meshing of the initial hull in blue and a deformed hull in red.

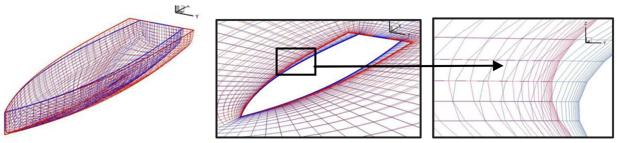

Figure 2: Initial and deformed meshes

Each deformation is defined by its "volume of action" and spatial functions. Three spatial functions define the displacement of the hull control points, depending on their x, y, z position. These functions are defined using 1 to 5th order Splines. Each transformation is monitored by the amplitude of the spatial functions, its "volume of action" remaining unchanged. Figure 3 shows a function which modifies the front sections fullness. The original section in the middle is black, negative amplitude leads to a narrower V shaped section in blue, positive amplitude creates a wider U shaped section in red. More details about this tool can be found in [5].

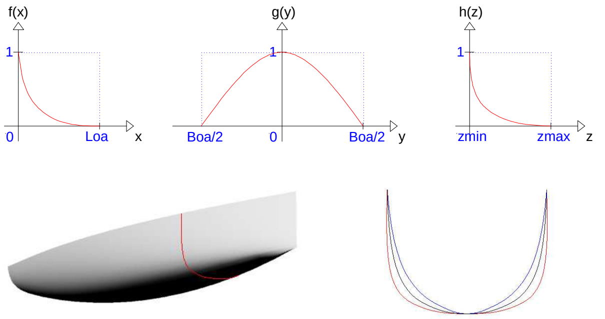


Figure 3: Definition and visualization of a transformation

## 2.3 HYDROSTATIC MODULE

A hydrostatic module has been developed specifically for this study. In fact, the characterization of the wetted shape of sail boat hulls under various hydrostatic equilibriums is the key of the chosen approach. In fact, as highlighted in [4], the measurements of the wetted shape under heel allow significant improvements in the accuracy of the prediction.

### 2.3.1 Adaptation of classical measurements

As we are dealing with asymmetrical wetted shapes, even the classical measurements have to be redefined.
Once the hydrostatic equilibrium is achieved in the flow referential R0, i.e. $L_{CB}=L_{CG}$ and weight=displacement, the apparent leeway angle ALA is computed. This angle is quoted in green in Figure 4 and defined in the next section. Once ALA is computed, a new referential R1 is defined as a rotation of R0 around Z0 axis. The rotation value is ALA, so that the wetted shape is aligned with the X1 axis. All the measurements such as waterline beam and length, master section area, prismatic coefficient and so on are then carried out in the R1 referential.

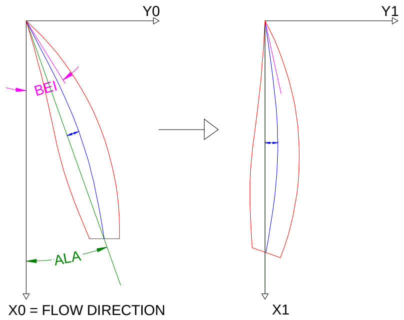


Figure 4: Measurements of asymmetrical wetted shapes

### 2.3.2 Parameters quantifying the asymmetry

Three measurements depicted on figure 4 were defined in order to characterize the asymmetry.

- The apparent leeway angle, ALA. The points A and B are defined as the centre of the sections situated respectively at 5% and 95% $L_{WL}$. ALA is the angle between (AB) and the direction of the incoming flow.
- The bow entry incidence, BEI defined as the angle between the bisectrix of the water plane entry and the direction of the incoming flow.
- The relative camber, defined by the deviation of the mean line of the water plane divided by LWL.

### 2.3.3 Additional hydrostatic parameters

The pressure field and the hydrodynamic drag of the tested hulls present a high sensitivity to the longitudinal shape of the hull. Some measurements such as the rocker angle R were defined as shown in Figure 5 to characterize the keel line. Regardless the heel value, these angles and immersions are always measured in the vertical plane (X1, Z0) in which the hull has the larger lateral area.

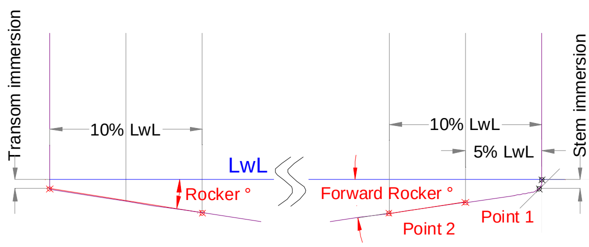


Figure 5: Measurements of the keel line

2.4. RANSE SOLVER

ICARE [6] is a RANSE (Reynolds Average Navier-Stokes Equations) free-surface solver initially co-developed by Ecole Centrale Nantes under French Ministry of Defence support, and by Hydrocean. It uses the k-ω turbulence model developed by Wilcox [7]. The free surface is described by an interface tracking method. General schemes are based on second order (in space and time) implicit finite differences. Discrete unknowns are distributed on a hexahedral structured curvilinear grid fitted to the hull and the free surface.
The interface tracking approach allows a very a good precision/time ratio and is also very suitable for the construction of a systematic series. The drawback of this mesh deformation approach is its inability to describe breaking waves. This reduces the maximum Froude number to about 0.6 to 1.0, depending on the hull shape.
A satisfying validation of the ICARE code on sailing yacht hulls has been performed. As part of collaboration with the Delft Ship Hydromechanics Laboratory, J.A. Keuning and his team made available the detailed tank test results of three different models of the DSYHS. The length to displacement ratios vary from 5 for model 23 to 7 for Model 28. Results on bare hull but also on appended hulls were available. ICARE computations on both bare and appended hull were performed. The computations were carried out at model scale, with semi captive method. On the three models, the agreement between the tank tests and the RANS solver was good, within the 5% range concerning drag and showing the same behaviour concerning the heave and trim over the whole speed range. The results concerning Model 25 are presented in Figure 6. Error bars have been represented with a 0.5 N measurement uncertainty plus a 5% margin to help the reading of the discrepancies.

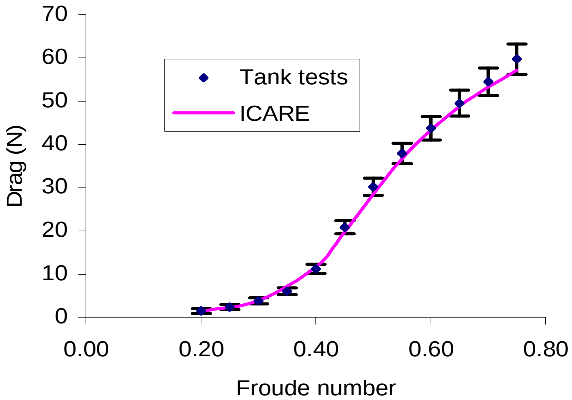


Figure 6 : ICARE solver validation - DSYHS Model 25

Satisfying results were also obtained and published in [8] concerning validation of the ICARE solver on an IMOCA 60 hull.

## 3. DATABASE AND REGRESSION BUILDING

In the field of statistics and data mining, a lot of the knowledge and tools were developed to process real life data, such as demographical, economical or medical figures. Here, we have the luck to control most of the data we will process in the end. In fact, a database made of numerical simulations is in a way the exact opposite of a real life database. Not only we control most of the explanatory variables value of our experiments as in a laboratory, but we have a 100 % repeatability of the experiments. This does not mean that the result is perfect, but from a statistical point of view, it is very different from real life experiments. It is luck, but it is also additional work. The data does not exist, we need to build it and find a satisfying way of building it.

### 3.1 DATABASE BUILDING – DESIGN OF EXPERIMENTS

Once the extreme values of the inputs variables are defined, there are many ways to design the experiments, i.e. define the number of points needed in the database and their spacing with respect to the sensitivity of the response (outputs) is a complex problem. The aim is to extract as much of the physics as possible with a minimum number of experiments. In our case, the input variables are the magnitude of the transformations applied to the parent hull and the computational parameters such as speed, weight and $LC_G$. Once a range and a step of variation have been defined for each input variable, the straight forward approach is to follow a full factorial design of experiments. In our case, we have at least 10 input variables. If we want to explore at least three different values for each variable, this leads to $3^{10} = 6.10^4$ computations, which is not realistic in our context. Several methodologies have been developed to reduce the number of experiments needed before the beginning of the experiments and the building of the model. We can quote the following methods: Reduced Factorial, , Box-Behnken, Latin Square, Taguchi Matrix.
The general idea is to assume some properties in the data and use them to reduce the number of experiments. Some methods assume linear or quadratic response in the data; others neglect the interaction between the explanatory variables, etc. A very good overview of the quoted methods and their applications can be found in [9], dealing with most of the classical statistical methods. Another interesting paper by Astrid Jourdan [10] deals more specifically with the design of experiments applied to numerical simulations with approaches allowing more flexible responses such as the Kriging technique. In our case, the design of experiments can be adapted as the database grows. We do not need to follow a plan defined a priori. In fact, the automated post treatment of the solver’s solution makes the results of each experiment immediately available in the database. It is worth to exploit the information collected about the response in order to figure if there are portions of the experimental region which could require a denser sampling than others. The design of experiments is realized in two steps. The first step can be described as exploration and the second one is the refining of the database.

#### 3.1.1 Exploratory design – Sobol sequence

Several methodologies have been developed to optimize the exploration phase. The goal is to provide a first response surface that will be the starting point of the refining phase. The response surface has to be defined on its whole range of variation and the points have to be distributed as evenly as possible. A specific structure in the repartition of the variables values may lead to a false interpretation of the response. A random sequence could be used but it tends to generate concentration of points in the same region, leaving other regions empty. Figure 8 shows how the Sobol sequence improves the repartitions of the variables values compared with a random sequence on a simple two dimensional case.

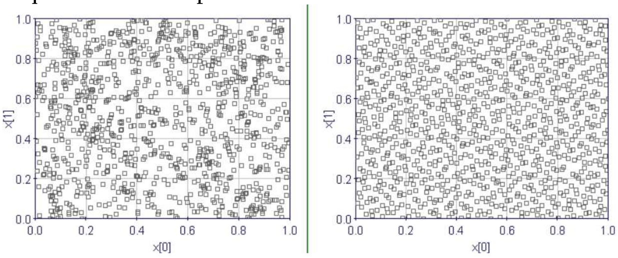

Figure 8: 1000 points generated with a random sequence on the left and a Sobol sequence on the right

The Sobol sequence has been chosen as initial design of experiments in this study. This sequence is widely used in the exploration phase, to initiate an optimization process for example. In the present work, the goal is not only to find the optimum of the response surface but to characterize it as well as possible in a given time lapse.

3.1.2 Database enhancement – Lipschitz sampling

One of the most promising approaches to refine a response surface is called Lipschitz sampling [11]. Once a first response surface has been defined, the algorithm computes a scalar called Lipschitz constant quantifying the local complexity the surface. This constant is regularly recomputed on the whole surface to readjust the choice of the next experiments and the high gradient zones become more and more well defined as the database is built. Figure 9 shows a typical case of application. X and Y represent two explanatory variables and Z is the response variable. From a initial response surface, the algorithm has refined around the break line to allow a very satisfying modelling of the response.

The Y vs. X graph on the left of figure 9 illustrates the behaviour of the algorithm. The original average density of points was 5 points per unit in the X direction and 4 points per unit in the Y direction. This density has been increased by the algorithm in both directions up to 20 points per unit in the "break" region.

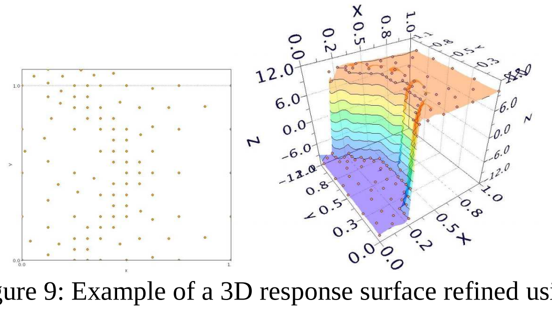

Figure 9: Example of a 3D response surface refined using Lipschitz sampling (Y vs. X graph on the left)

This algorithm highlights one of the main advantages of a completely numerical approach to build a systematic series: the ability of following an adaptable design of experiments, which is more and more relevant as the database grows. The experiments have no longer to be designed a priori, assuming properties in an unknown data base.

## 3.2. REGRESSION BUILDING – VARIABLE SELECTION

In this section, the goal is to identify the relevant relations between the predictive variables on one side (the attitude variables and geometrical measurements computed by the hydrostatic module) and the dependant variables on the other side (the hydrodynamic forces and running attitude). What is a "relevant relation"?

The literature on naval hydrodynamics shows that the purposes motivating regression analysis may differ largely; the qualities sought after in the regressions will vary accordingly.

The regression analysis can be used to build a very simple model, with focus on the reduction of required predictors and a low constraint on accuracy, in order to reduce the number of required measurements to predict a given quantity.

In our case, unlike twenty years ago, the hydrostatic computations and measurements are quasi instantaneous, the number of predictive variables will therefore not be reduced to avoid fastidious measurements. This number will be a compromise between accuracy and robustness. Too few predictive variables will lead to a lack of sensitivity and therefore to obsolete regressions. If too many variables are to be introduced, the regression parameterization will be unstable; mainly due to multi collinearity between the predictors. Multi collinearity is a linear relationship between two or more predictive variables. In the presence of multi collinearity, the value of the coefficient estimates $a_i$ associated to the collinear predictors may change erratically in response to small changes in the model or the data. A small change in the sample will cause a large variation of $a_i$, which is to be avoided as the $a_i$ value should give relevant information on the effect of the associated predictor.

The choice of the relevant predictors is therefore one of the keys of this study.

The multi collinearity has to be avoided above all. The correlation between the predictors has to be kept as low as possible. Each independent variable should have a non-zero correlation coefficient at a high significance level (low p-value). It should not be possible to significantly improve the accuracy of the regression by introducing extra independent variables. It should not be possible to exclude a predictor without significantly reducing the accuracy of the regression.

Several statistical tools have been tested in order to build multivariate regressions and avoid multi collinearity as far as possible. A simple and satisfying approach is the forward selection algorithm.

**Forward selection algorithm**
This algorithm will produce a multiple linear regression to explain a dependent variable based on independent variables that will be selected during an iterative process. The selection methodology is based on partial correlation computations.

- It starts with the best linear fit using the most correlated variable.
- Then the partial correlation of the remaining predictors is computed (i.e. their correlation to the residuals of the first regression). The variable showing the highest partial correlation is selected. This new variable is added in the regression and the residuals recomputed.
- This is repeated until the p-value of the test of significance of remaining variables is below a specified significance level.

A more detailed description of the variable selection methodology is available in [5].

## 4. PROPOSED FORMULATIONS

In order to provide a representative but synthetic example of the proposed methodology, a specific database has been created around the Volvo 70 rule.

### 4.1 GENERATION OF THE DATABASE

#### 4.1.1 Description of the geometries

From a parent design, two initial hull shapes are extracted. The first one is the upright hull; the second one is derived from the wetted shape of the heeled hull (20 degrees heel angle). Figure 10 shows four random hulls in the series, two symmetrical hulls on the left and two asymmetrical hulls on the right.

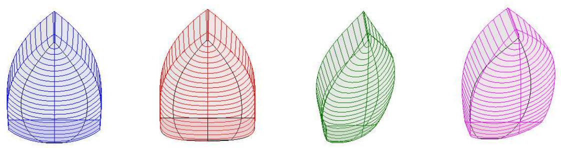

Figure 10: Four random hulls of the Volvo 70 series

These hulls and the corresponding meshes are generated using the presented morphing tool. Eight different geometrical transformations are defined and applied at various magnitudes to generate 250 different hulls. These transformations must generate realistic hull shapes but also maximize the changes in the physics of the flow to give as much information as possible on the design space. The choice of the transformations is guided by the experience of designing hulls by hand and by the literature which highlighted some relevant hydrostatic parameters to be varied. In fact, the computer has to reproduce what is carried out by hand during a typical preliminary design phase, producing a wide range of realistic hull shapes in order to understand as well as possible the design trade offs of the project.
The volume of action of the six deformations includes the whole hull. Two deformations concern the shape of the fore sections of the hull, two other the stern sections. Those transformations are modifying the beam, draft and fullness of the sections. The longitudinal repartition of each transformation is smoothed using Bezier functions.
Every transformation is carried out under hydrostatic constraints. For example, when the beam of the fore sections is increased, their draft is automatically reduced to keep the same longitudinal volume repartition.
The two last transformations concern solely the asymmetrical hull shapes. They change the leeway and the longitudinal curvature of the immersed part of the hull in the transverse direction. This allows various combinations of ALA, BEI and relative camber to be generated. More details about those transformations can be found in [5]. Figure 11 gives the range of variation and the distribution of some of the main hydrostatic parameters used in the regressions.

| | min | max |
|---|---|---|
| ALA (°) | -12 | 12 |
| BEI (°) | -15 | 15 |
| ie (°) | 15 | 54 |
| $C_P$ | 0.52 | 0.66 |
| $C_B$ | 0.35 | 0.48 |
| $C_{flot}$ | 0.62 | 0.82 |
| $C_M$ | 0.64 | 0.75 |
| $L_{CB}$ | 0.518 | 0.64 |

| | min | max |
|---|---|---|
| R (°) | 1.2 | 6.2 |
| FR (°) | -6.3 | -2 |
| $X_T/L_{WL}$ | 0.38 | 0.65 |
| $L_WL/ L_{OA}$ | 0.9 | 1 |
| $I_S/T$ | 0 | -0.45 |
| $S_T/S_{MS}$ | 0 | 0.5 |
| B/L | 0.12 | 0.2 |
| B/T | 3.2 | 12 |

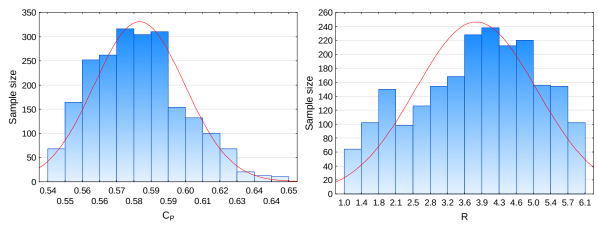


Figure 11: Range of variation of some geometrical measurements (top) and distribution of Cp (bottom left) and Rocker angle (bottom right)

A Gaussian fit is represented in red on the histograms to illustrate the gap between the distribution of the considered explanatory variable and a normal distribution. It allows a synthetic overview of the distribution of the variables. In the present case, the geometrical transformations cover a wide range of Cp and Rocker values with a satisfying distribution.

#### 4.1.2 Testing conditions

The geometries are tested at three different speeds, 10, 14 and 18 knots. The computations are carried out at real scale, with boats of 21.5 m overall length. The boats are free to heave and trim. The sail centre of effort is situated 13.5 m above the water plane. The longitudinal position of the centre of gravity of the boat is varied among three different values: 11.2, 11.8 and 12.4 m (i.e. $L_{CB}/L_{OA}$=0.52, 0.55 and 0.58). The transition of the boundary layer is forced at the bow of the boat, so that the flow is fully turbulent. All the forces are expressed in

$R_0$. The moments are computed with respect to the centre of gravity. This database is made of 2250 computations (250 shapes x 3 $L_{CG}$ x 3 speeds).

## 4.2 FORMULATIONS

The formulations are speed dependent; meaning that each speed has its associated set of estimates (or regression coefficients). All the forces and attitudes are expressed in R0. The trim angle is indeed computed in the water referential, y0 axis being perpendicular to the incoming water flow and normal to the water surface.
As described before, we use generalized linear regressions to approximate the quantities. This means that each quantity is expressed as the weighted sum of explanatory variables or the weighted sum of combination of explanatory variables. Once one of the response variables is formulated, it is a combination of explanatory variables and thus might be used in the formulation of second response variable.
On the bright side, this "encapsulation" might enhance the formulation of the second response variable and also facilitate the understanding of the physics. On the dark side, this decreases the stability of the formulation, by summing the errors. At this stage, it was felt that a trial and error approach would be valuable, in order to have an overview of the potential gain in accuracy allowed by the different encapsulation orders compared with no encapsulation at all. The forward selection algorithm was run several times for each response variables leaving access to other response variables or not. The resulting chosen order is presented hereafter.
The numerical values of formula's coefficients are regrouped in figure 13.
A much more detailed analysis and interpretation of the following formulations is available in [5].

### 4.2.1 Side force generation

The following expression gives a good approximation of the side force production:

$$\widetilde{Fy} = a_1 ALA + a_2 ALA^3 + a_3 BEI + a_4 CBR$$

Where:

$$\widetilde{Fy} = \frac{Fy}{A_{HL} \cdot \frac{1}{2}\rho . V^2}$$

### 4.2.2 Pressure drag

Numerical codes compute total resistance as the sum of the pressure drag (normal forces) and frictional drag (tangential forces); it seems therefore natural to use this decomposition to build the formulations.

$$Fx = Fpx + Ffx$$

As the displacement variations of the hulls in the considered database are relatively small, a simple non dimensional form has been used:

$$\widetilde{Fpx} = \frac{Fpx}{Fz} . \left(\frac{L_{WL}}{\nabla^{1/3}}\right)$$

The pressure drag is one of the hardest quantities to model on a sailing yacht. Several physical effects are involved and their contribution to the total drag is highly dependant on the Froude number and the Reynolds number. This explains why numerous variables are used in the following expressions; however Figure 13 shows that some variables are not used at every speed, the corresponding coefficient being null.

$$\widetilde{Fpx} = b_0 + b_1 . \frac{L_{WL}}{\nabla^{1/3}} . \frac{Fy}{Fz} . \widetilde{Fy} + b_2 . ALA^2 + b_3 . C_P + b_4 . C_P{}^2 + b_5 . \frac{L_{CX}}{L_{WL}} + b_6 . \left(\frac{L_{CX}}{L_{WL}}\right)^2$$

$$+ b_7 . \frac{L_T}{L_{WL}} + b_8 . \frac{L_T}{L_{WL}}^2 + b_9 . \frac{T}{L_{WL}} + b_{10} . C_{Pfront} + b_{11} . C_{Pfront}{}^2 + b_{12} . C_X + b_{13} . C_X{}^2 + b_{14} . R$$

It is interesting to plot contribution of the $C_P$ terms for different values of $C_P$ at the three speeds. The contribution is the value of the sum ($b_3 . C_P + b_4 . C_P^2$), this sum changes the value of the pressure drag depending on the $C_P$ value.

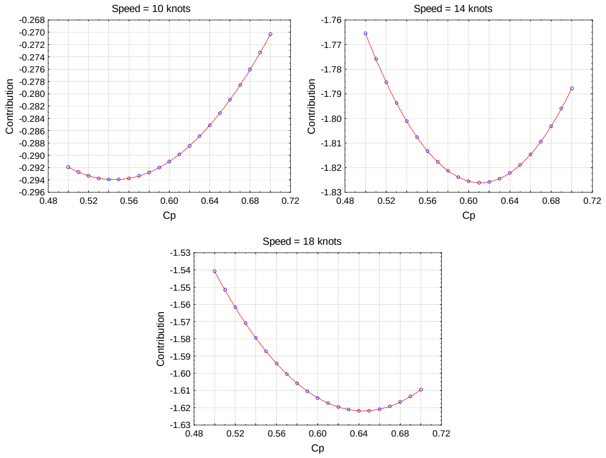


Figure 12: Contribution of Cp to Fpx depending on the Cp value at 10 kts (top left), 14 kts (topright) and 18 kts (bottom)

Figure 12 shows a very consistent behaviour of the pressure drag formulation, being in the trend of what can be read in the literature on naval hydrodynamics.
At 10 knots, or Fn=0.35, the optimum $C_P$ lies around 0.54. At 14 knots, or Fn=0.5, the optimum $C_P$ lies around 0.61.At 18 knots, or Fn=0.65, the optimum $C_P$ lies around 0.64. As for $C_P$, most of the expressions are quadratic with a positive value of the estimates of the squared term. This allows an optimisation process without ending "in the corners".

### 4.2.3 Running trim

The running trim is defined as the change in trim angle between the hydrostatic position at the considered heel angle and the trim angle reached at the considered Froude number.

$$Roy = c_0 + c_1 . \frac{Fpx}{Fz} + c_2 . \frac{L_T}{L_{WL}} + c_3 . \frac{L_{BWL}}{L_{WL}} + c_4 . \frac{L_{CB}}{L_{WP}} + c_5 . \frac{T_T}{T} + c_6 . R$$

This approximation of the running trim is very promising. It allows the coupling with an appendage model, providing the proper angles of incidence of the lifting devices fitted on the hull.

### 4.2.4 Running sinkage

The running sinkage is defined as the change in sinkage of the centre of gravity between the hydrostatic position at the considered heel angle and the sinkage reached at the considered Froude number.

$$\widetilde{Trz} = d_0 + d_1.C_B + d_2.C_{WP} + d_3.\frac{L_{BWL}}{L_{WL}} + d_4.ALA^2$$

Where $$\widetilde{Trz} = \frac{Trz}{T}$$

### 4.2.5 Frictional drag

$$\widetilde{Ffx} = e_0 + e_1.\widetilde{Trz} + e_2.Roy + e_3.C_{WP} + e_4.C_{Pfront} + e_5.|ALA|$$

With $$\widetilde{Ffx} = \frac{Ffx}{C_f.\frac{1}{2}.\rho.V^2.S_C}$$

$C_f$ is determined using the ITTC 57 extrapolation line; based on the hydrostatic waterline length.

As $S_C$ is the static wetted surface of the hull, $\widetilde{Ffx}$ contains the variations of wetted surface due to the dynamic position of the boat and the free surface deformations. A fraction of the form coefficient is also contained in $\widetilde{Ffx}$, leaving the other fraction in the pressure drag.

### 4.2.5 Yaw moment

The yaw moment is computed in $R_0$, with respect to the centre of gravity. This moment can be split into two components:

– A component coming from the drag force, multiplied by the lever between the centre of gravity and the centre of effort of the drag.
– A component coming from the side force, multiplied by the lever between the centre of gravity and the centre of effort of the drag.

On most of the mono hulls, the component coming from the drag forces is very small compared with the component coming from the side force, except when the side force is very small. In this case, the yaw moment is also very small and its approximation is useless. The sample used to approximate the yaw moment has been selected using the following criteria:

$$\left|\frac{Fy}{Fpx}\right| \geq 5\%$$

The following expression has been used to determine the longitudinal position of the side force centre of effort with respect to the centre of gravity, often called centre of lateral resistance (CLR).

$$L_{CLR} = \frac{Mz}{Fy}$$

The following expression gives a good approximation of the scaled centre of effort position.

$$\widetilde{L_{CLR}} = f_0 + f_1.\frac{Trz}{L_{WL}} + f_2.|BEI| + f_3.BEI^2 + f_4.C_B + f_5.\frac{L_{CX}}{L_{WL}} + f_6.\frac{B_{WL}}{L_{WL}}$$

With $$\widetilde{L_{CLR}} = \frac{L_{COE}}{L_{WL}}$$

| Fn | Speed (kts) | a1.10^3 | a2.10^6 | a3.10^3 | a4.10^3 | R2 |
|---|---|---|---|---|---|---|
| 0.35 | 10 | -0.71 | -3.88 | -0.53 | | 0.99 |
| 0.50 | 14 | -2.97 | -3.44 | -0.24 | | 0.98 |
| 0.65 | 18 | -2.87 | -6.24 | | -107 | 0.98 |

| Fn | Speed (kts) | b0 | b1 | b2.10^3 | b3 | b4 | b5 | b6 | b7 |
|---|---|---|---|---|---|---|---|---|---|
| 0.35 | 10 | 1.88 | 15.04 | 0.10 | -1.08 | 0.99 | -3.36 | 2.99 | 0.18 |
| 0.50 | 14 | 5.13 | 6.55 | 0.52 | -5.97 | 4.88 | -7.64 | 6.92 | -0.35 |
| 0.65 | 18 | 4.19 | 4.40 | 0.90 | -5.04 | 3.91 | -5.30 | 4.94 | -0.44 |

| Fn | Speed (kts) | b8 | b9 | b10 | b11 | b12 | b13 | b14 | R2 |
|---|---|---|---|---|---|---|---|---|---|
| 0.35 | 10 | -0.13 | -0.35 | -2.60 | 2.64 | | | | 0.83 |
| 0.50 | 14 | 0.33 | 6.08 | -4.23 | 4.20 | | | | 0.98 |
| 0.65 | 18 | 0.32 | 7.28 | | | -3.14 | 2.54 | 0.01 | 0.99 |

| Fn | Speed (kts) | c0 | c1 | c2 | c3 | c4 | c5 | c6 | R2 |
|---|---|---|---|---|---|---|---|---|---|
| 0.35 | 10 | -2.61 | -24.67 | 0.65 | 0.85 | 1.98 | 0.01 | 0.00 | 0.93 |
| 0.50 | 14 | -1.33 | -8.56 | 0.32 | 0.73 | 1.13 | -0.38 | 0.12 | 0.91 |
| 0.65 | 18 | -0.52 | -2.05 | 0.70 | 0.73 | 0.22 | -0.28 | 0.13 | 0.90 |

| Fn | Speed (kts) | d0.10^3 | d1 | d2 | d3 | d4.10^3 | R2 |
|---|---|---|---|---|---|---|---|
| 0.35 | 10 | -35.95 | -0.50 | 0.26 | -0.07 | -0.31 | 0.85 |
| 0.50 | 14 | 30.49 | -0.80 | 0.31 | -0.13 | -0.84 | 0.81 |
| 0.65 | 18 | 43.80 | -0.63 | 0.26 | -0.15 | -1.09 | 0.87 |

| Fn | Speed (kts) | e0 | e1 | e2.10^3 | e3 | e4 | e5.10^3 | R2 |
|---|---|---|---|---|---|---|---|---|
| 0.35 | 10 | 1.53 | -1.16 | 9.03 | -0.61 | 0.08 | 5.43 | 0.83 |
| 0.50 | 14 | 1.61 | -1.19 | -99.80 | -0.78 | 0.35 | 1.90 | 0.86 |
| 0.65 | 18 | 1.63 | -1.43 | -53.27 | -0.91 | 0.43 | 0.47 | 0.83 |

| Fn | Speed (kts) | f0 | f1 | f2.10^3 | f3.10^3 | f4 | f5 | f6 | R2 |
|---|---|---|---|---|---|---|---|---|---|
| 0.35 | 10 | -5.24 | 217.43 | 21.62 | 0.80 | 7.19 | 4.00 | 26.54 | 0.81 |
| 0.50 | 14 | -1.61 | 58.09 | 22.63 | -0.54 | 1.13 | 1.64 | 13.34 | 0.84 |
| 0.65 | 18 | -0.40 | 24.52 | 41.20 | -1.76 | -1.62 | 0.76 | 15.39 | 0.89 |

Figure 13: Estimates of the presented formulations

A detailed evaluation of the accuracy of these formulations is available in [5].

## 4. FORMULATIONS BENCHMARK

In order to evaluate the sensitivity and accuracy of the presented formulations, a candidate hull which wasn't part of the systematic series has been characterized with different tools at two speeds, 3 heel and 4 leeway angles. Four tools are compared:

– The RANS code ICARE.
– The RANS code Star CCM+.
– The DSYHS formulations as implemented in WinDesign VPP of the Wolfson unit [12].
– The presented formulations.

Due to the limited length of the paper, only two graphs are presented on figure 14. They present the changes in side force production and pressure drag of the bare hull with respect to changes of heel angle with zero leeway and 14 knots of boat speed. A more extended validation study is available in [4]. The forces are expressed in Newton and the angles in degrees. In the chosen referential, a positive side force is a force to windward.

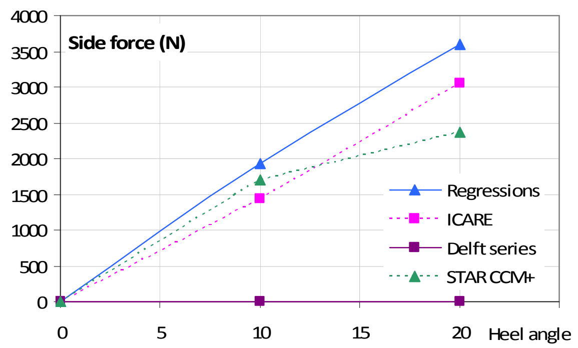

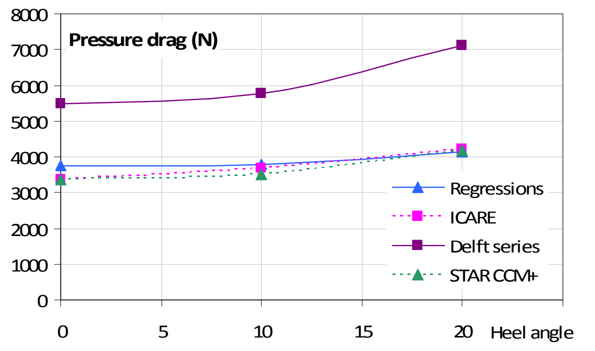


Figure 14: Side force and pressure drag predictions at 14 knots for different heel angles and no leeway.

With the exception of the side force at 14 knots, where the discrepancy reaches 25 %, the overall agreement between the two solvers is very good, despite very different computational methods; finite differences against finite volumes; interface tracking against interface capturing, etc. The discrepancy on side force at 14 knots might be related to bow wave effects. In fact, the bow region has a large contribution to side force and the bow wave is the most intense at this pre-planing speed.

The DSYHS show a 45 % overestimation of the upright pressure drag which means a 23% discrepancy on total drag. These figures confirm the results published in [8], where the DSHYS are compared with tank tests on an IMOCA 60 and show around 19 % overestimation of total drag at Fn=0.6. The influence of heel on side force production is not taken into account by the DSYS since the asymmetry of the heeled hull is not explicitly measured. The pressure drag sensitivity to heel is in the right trend, even though overestimated on this hull.

The presented regressions give very satisfying results, showing the appropriate trends on side force and pressure drag between the different heel and leeway angles. The absolute values given by the regressions are good, often under 5% and a maximum of 15 % discrepancy compared to ICARE computations. Further work includes new series and associated formulations to tackle more various hull shapes, including larger displacement to length ratios. This will be a step towards more versatile formulations, which will be compared with the DSYHS on some of the models of the Delft series.

## 5. INTEGRATION IN A VPP – FIRST RESULTS

The current ongoing work concerns the development of a VPP able to take advantage of the presented formulations. Two separated models are used in addition to the presented formulations for bare hulls: an appendage model based on the lifting line theory [13] and an aerodynamic model based on the Offshore Racing Committee model [12]. This VPP finds the equilibrium between the forces computed by three models on the six degrees of freedom of the boat. It solves the equilibrium equations to find the heel, speed, leeway, running trim and rudder angle fulfilling the best equilibrium between all the forces. The "best" equilibrium is found when the boat speed is maximum in a given true wind speed and wind angle. An apparent weight of the boat carried by the hull is also computed, accounting for the appendages and sails contributions on the vertical axis z0.

This VPP allows a very fast evaluation or optimization of fine tunings such as dagger-boards toe-in or keel tilt angle. The keel tilt is defined as the angle between the rotation axis of a canting keel and the horizontal axis when the boat is in its hydrostatic equilibrium upright. This tilt angle introduces a coupling between the cant angle and the keel angle of incidence. A positive tilt (forward bearing moved upwards) tends to generate lift on the keel fin (positive side force and upwards lift), modifying the running trim and sinkage of the hull as well as the leeway angle and the yaw equilibrium, see figure 15.

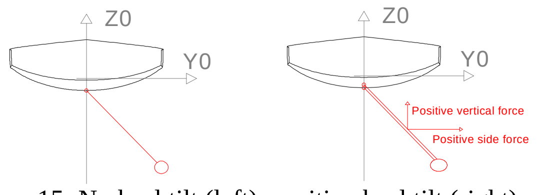


Figure 15: No keel tilt (left), positive keel tilt (right)

In order to test the sensitivity of the recently developed VPP, the influence of the keel tilt on the equilibrium of a Volvo 70 is investigated. The keel is canted 40 degrees to windward, the leeward rudder 15 degrees to leeward and the dagger boards are lifted out of the water. This typical broad reaching configuration is studied with full mainsail and a fractional headsail from true wind angle of 110 to 140 degrees. Figure 16 presents the boat speed, displacement carried by the hull, running trim and leeway angle for 3 different keel tilt angles in 12 knots of true wind speed. On the presented configuration, the keel fin centre of surface is placed 1.15 m in front of the yacht centre of gravity.

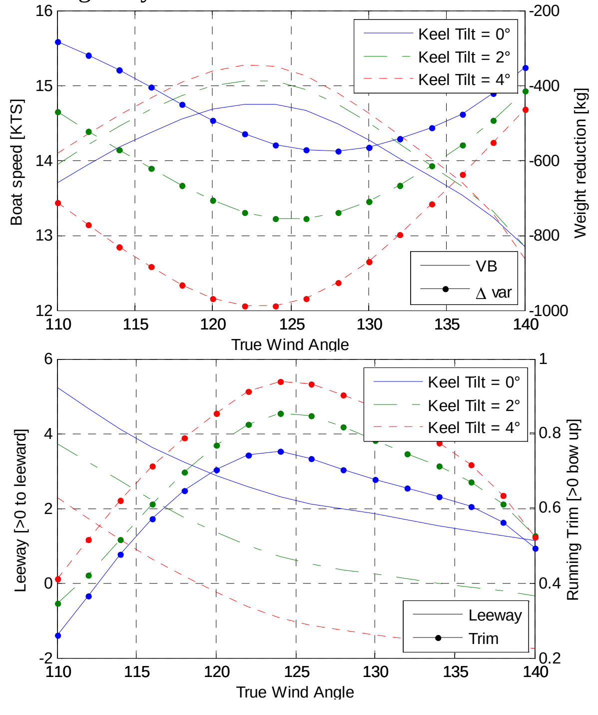


Figure 16: Speed, weight reduction (top), running trim and leeway angles (bottom) for 3 different keel tilts.

The results show a very satisfying sensitivity to the change in keel tilt, showing large changes in the vertical and horizontal forces generated by the appendages. The trends are good, high values of keel tilt leading to significantly reduced apparent weight and leeway angles. The apparent weight carried by the hull is reduced by 500 kg with a keel tilt of 4 degrees compared with no keel tilt. The leeway angle is reduced by almost 2 degrees. The resulting changes in maximum boat speed are not negligible, up to 0.5 knots. The boat speed and true wind angle are expressed with respect to the course of the yacht (water flow referential), not its longitudinal axis (boat referential).

The presented coupling between hull and appendage models neglects their hydrodynamic interaction. In fact, the flow around the hull is indeed modified by the presence of the appendage and the hull changes the behaviour of the appendages. The model might therefore be enhanced by introducing corrective terms to take this interaction into account, based on appended computations or tank tests. It is part of the ongoing work. As this interaction is highly dependant on the distance between the appendage root and the free surface, the running trim and running sinkage formulations presented in this report will be used to compute the free surface proximity. It must be mentioned that this interaction phenomenon is much weaker on modern yachts than in the past mainly due to the high aspect ratio of the appendages. Modern appendages present much smaller volume close to the hull and therefore weaker interaction with hull and the free surface.

## 6. CONCLUSION

A complete methodology to study the hydrodynamic behaviour of yacht hulls was presented. First step is the database building: choice of the experiments, generation and measurement of the geometries, meshing and finally computation using a RANSE code; second step is the statistical methodology to treat the database. An effort is made in this article to detail this methodology to allow its application to other fields. New formulations for the approximation of the forces production and attitudes of bare hulls in calm seas have been presented. A specific VPP has been developed to use these formulations and the first results of the coupling with the appendage and aerodynamic models are very promising.

## ACKNOWLEDGEMENTS

Gianluca Guelfi from the University of Genoa is gratefully acknowledged for his work on the VPP, implementing lifting line theory, aerodynamic model and optimization algorithms. Hydrocean is also to be acknowledged concerning the development of the morphing tool used in the database building loop. Finally, the authors would like to thank all the members of Marc Lombard Yacht Design Group for their support and the funding of this research program.

## AUTHOR' BIOGRAPHY

**L. Huetz** currently works at Marc Lombard Yacht Design Group. He is responsible for performance studies, hull design and optimization. He obtained his PhD. at Ecole Centrale de Nantes in 2012.

## REFERENCES

1. JA. Keuning, U.B. Sonnenberg, "Approximation of the hydrodynamic forces on a sailing yacht based on the Delft Systematic Yacht Hull Series". *The International HISWA Symposium on Yacht Design and Yacht Construction*, 1998
2. JA. Keuning, M Katgaert, "The bare hull resistance of the delft systematic yacht hull series at high speeds". *Proceedings of the 1st Innovsail Conference, Lorient*, 2008.
3. L. Huetz, B.Alessandrini, "Systematic study of the hydrodynamic forces acting on a sailing yacht hull using parametric design and CFD", *Proceedings of OMAE,, Rotterdam, The Netherlands,* 2011
4. L. Huetz, Y. Andrillon, P.E. Guillerm, B. Alessandrini, "Systematic study of the hydrodynamic forces on a Volvo 70 yacht using parametric design CFD and variable selection, *4th High Performance Yacht Design Conference, Auckland, New Zealand*, 2012.
5. L. Huetz, "Systematic study of the hydrodynamic behaviour of sailing yachts hulls". *PhD. Thesis. Ecole Centrale de Nantes*, 2012.
6. B. Alessandrini, G. Delhommeau, Simulation of three-dimensional unsteady viscous free surface flow around a ship model". *International Journal for Numerical Methods in Fluids, vol 19, pp 321-342,* 1994.
7. D. C. Wilcox, November, "Multiscale model for turbulent flows". *AIAA Journal Vol 26, pp. 1211-1320*, 1988.
8. J. Raymond, "Performance estimation of planing yachts". *PhD Thesis, Ecole Centrale de Nantes,* 2009.
9. NIST/SEMATECH, "E-Handbook of Statistical Methods", http://www. itl.nist.gov/div898/handbook, 2012.
10. A. Jourdan, "Planification d'expériences numériques". *Revue MODULAD*, 2005.
11. A. Lovison, "Lipschitz Sampling for Improving Metamodels in modeFRONTIER". *Technical report, ESTECO*, 2008.
12. ORC VPP Documentation 2012.
13. J. Katz, A. Plotkin, "Low speed aerodynamics". *McGraw – Hill*, 1991.